PriMera Scientific Engineering
Volume 9 Issue 1 July 2026
ISSN: 2834-2550

PriMera Scientific Publications

Rambling and Trembling as Distinct Components of the Closed Postural Control Circuit: Multi-Sensor Wearable Validation of a Hierarchical Decomposition Mechanism

Type: Review Article
Received: May 05,2026
Published: June 30, 2026

Citation:
Kundai Farai Sachikonye. "Rambling and Trembling as Distinct Components of the Closed Postural Control Circuit: Multi-Sensor Wearable Validation of a Hierarchical Decomposition Mechanism". PriMera Scientific Engineering 9.1 (2026): 34-50.

Kundai Farai Sachikonye*

AIMe Registry for Artificial Intelligence, Germany

***Corresponding Author:** Kundai Farai Sachikonye, AIMe Registry for Artificial Intelligence, Germany.

Abstract

The rambling-trembling decomposition of the center-of-pressure (CoP) trajectory during quiet standing separates slow supraspinal drift (*rambling*) from fast peripheral oscillation (*trembling*). The decomposition is empirically robust, has substantial clinical reproducibility, and is sensitive to cognitive load, aging, and neurological disease, yet a quarter century after its introduction [Zatsiorsky and Duarte, 2000] it remains mechanistically unexplained. Alternative theories variously interpret the two components as stochastic versus deterministic, neural versus passive, or central versus peripheral, but none account for the full set of observations: (i) rambling and trembling exhibit different power spectra and different sensitivities to dual-task interference; (ii) aging preferentially affects trembling bandwidth; (iii) Parkinson's disease, cerebellar ataxia, and vestibular loss each produce characteristic rambling-trembling signatures that are dissociable; (iv) deafferented patients exhibit total loss of both components on eye closure. We propose that rambling and trembling are two levels of the same closed postural control circuit operating at different time scales: rambling is the low-frequency charge redistribution at supraspinal nodes (primary motor cortex, cerebellum, vestibular nuclei, brainstem) that biases the closure condition of the spinal postural loops; trembling is the high-frequency bounded oscillation of the spinal loops (stretch reflex, Ib inhibition, reciprocal inhibition) that maintain balance about that biased configuration. The two components are coupled through descending and ascending pathways whose integrity governs their mutual phase relationship. This picture predicts the observed spectral separation, the dual-task and aging effects, the pathology-specific signatures, and the vestibular-loss phenomenology. We develop the prediction quantitatively, specify a multi-sensor wearable protocol (smartphone/smartwatch inertial measurement unit [IMU], photoplethysmography [PPG], wrist-worn electromyography [EMG], ankle-mounted force-sensing insole) for non-invasive extraction of both components, derive consistency conditions across sensors, and report validation results from numerical simulations that reproduce the spectral structure of human postural sway, the dual-task effect (40-55% sway increase under cognitive load), the rambling-trembling spectral separation (> 90% correlation

with ground-truth decomposition), and the predicted signatures of deafferentation, Parkinsonian rigidity, and cerebellar ataxia. The framework provides the first mechanistic derivation of the rambling-trembling decomposition, enables low-cost consumer-grade measurement of postural control components, and establishes specific clinical signatures with diagnostic value.

Keywords: postural control; rambling; trembling; quiet standing; wearable sensors; inertial measurement units; center of pressure; closed-loop motor control; dual-task; Parkinson's disease; cerebellar ataxia; consumer health technology

Introduction

The quiet-standing phenomenon

A healthy adult standing quietly on a force plate is not motionless. The center of pressure (CoP) under the feet oscillates continuously with root-mean-square excursions of 2-5 mm in the anterior-posterior (AP) plane and 1-3 mm in the medial-lateral (ML) plane, at frequencies spanning roughly 0.05-3 Hz [Winter et al., 1998, Maurer and Peterka, 2005]. Total sway path length over a 30-second trial typically reaches 25-55 cm. The subject perceives no movement yet produces tens of discernible postural adjustments per second when measured to sub-millimeter precision.

These oscillations are not noise. They are not residual tremor of unstable balance. They are a structured signature of an active, distributed control system operating continuously to maintain upright posture against the destabilizing torque of gravity acting on a body mass approximately 1 m above the ankle joint—an inverted pendulum whose passive stiffness is insufficient to stabilize it without neural feedback [Morasso and Sanguineti, 2002, Loram and Lakie, 2002].

The rambling-trembling decomposition

In 2000, Zatsiorsky and Duarte [Zatsiorsky and Duarte, 2000] introduced a decomposition of the CoP trajectory into two components. They defined an *instant equilibrium point* (IEP): at each instant during quiet standing, there exists a point on the support surface at which the horizontal shear force is momentarily zero. A body positioned with its CoP at the IEP at that instant would experience no horizontal acceleration. The IEP trajectory over time, denoted $CoP_{Ra}(t)$ and called the *rambling component*, captures the slowly drifting reference configuration of the balance system. The deviation of the actual CoP from the IEP trajectory, $CoP_{Tr}(t) = CoP(t) - CoP_{Ra}(t)$, is called the *trembling component* and captures higher-frequency oscillation about the momentary reference.

The decomposition has been extensively validated across populations and conditions [Duarte and Freitas, 2010, Slobounov et al., 2008, Zatsiorsky and Aruin, 1999]. Key empirical observations include:

- ***Spectral separation***. Rambling power is concentrated below ~ 0.5 Hz; trembling power extends from 0.5 to ~ 3 Hz.
- ***Dual-task sensitivity***. Cognitive load (mental arithmetic, working memory tasks) increases both components but preferentially increases rambling amplitude [Lajoie et al., 1993, Woollacott and Shumway-Cook, 2002, Pellecchia, 2003].
- ***Aging effects.*** Older adults show increased total sway, with trembling amplitude rising faster than rambling, and reduced coupling between the two components [Prieto et al., 1996, Maurer and Peterka, 2005].
- ***Parkinson's disease***. Patients show increased trembling with reduced voluntary rambling modulation [Mancini et al., 2011].
- ***Cerebellar ataxia***. Patients show erratic rambling with preserved trembling amplitude but loss of phase coherence [van de Warrenburg et al., 2005].
- ***Vestibular loss***. Patients maintain rambling pattern with visual input but show rambling disintegration on eye closure [Horak, 2006].
- ***Deafferentation***. Patients with complete large-fiber sensory neuropathy show loss of both components on eye closure, with immediate postural collapse [Cole, 1991, Lajoie et al., 1996].

The mechanistic gap

Despite two decades of empirical work, the question *what are rambling and trembling mechanistically* remains open.

Proposals have included:

- Stochastic walk plus stabilization [Collins and De Luca, 1993, Chow and Collins, 1995];
- Supervisory versus autonomic control [Loram and Lakie, 2002, Masani et al., 2003];
- Open-loop plus closed-loop decomposition [Zatsiorsky and Duarte, 2000, Collins and De Luca, 1994];
- Predictive feedforward plus reactive feedback [Peterka, 2002, Jeka et al., 2004].

Each captures aspects of the phenomenology but none predicts the full pattern: the specific spectral separation, the dual-task preferential rambling effect, the aging preferential trembling effect, and the dissociable pathological signatures. A unified mechanism remains unspecified.

The claim of this paper

We propose that rambling and trembling are the low-frequency and high-frequency components of a single closed postural control circuit in which charge redistribution is hierarchically organized across time scales. Rambling reflects slow redistribution at supraspinal nodes (cortex, cerebellum, vestibular nuclei, brainstem) that biases the closure condition of spinal postural loops. Trembling reflects the bounded oscillation of those spinal loops about the momentarily biased configuration. The coupling between the two components is mediated by descending and ascending pathways whose integrity determines their mutual phase relationship.

This view predicts:

1. Distinct frequency bands reflecting the different time constants of supraspinal and spinal charge redistribution.
2. Increased cognitive load diverts supraspinal charge capacity, weakening the bias signal to spinal loops and increasing rambling amplitude preferentially.
3. Aging reduces spinal loop gain (via motor unit loss and receptor attrition), widening trembling bandwidth and amplitude.
4. Parkinson's disease impairs basal ganglia selection of supraspinal programs, reducing rambling modulation and permitting unregulated trembling amplification.
5. Cerebellar lesions disrupt phase coherence between supraspinal and spinal components without necessarily changing their amplitudes.
6. Vestibular loss removes one of the supraspinal input channels, degrading rambling specifically when alternative channels (vision) are unavailable.
7. Deafferentation breaks the closure of the spinal loops entirely, eliminating both components.

Each prediction matches established empirical findings without parameter tuning. Moreover, the mechanism suggests that rambling-trembling analysis need not rely on specialized force plates: any sensor measuring body-sway proxies at appropriate bandwidth should recover both components, with consistency across sensors providing a non-invasive validation unavailable to single-sensor protocols.

Wearable multi-sensor validation

We validate the framework through multi-sensor measurement using consumer-grade devices: smartphone or smartwatch inertial measurement units (IMU) for body sway, photoplethysmography (PPG) for cardiac coupling (rambling has known cardiorespiratory correlates [Bonnet and Despretz, 2012, Hunter and Kearney, 1981]), wrist EMG patches for motor unit activity during quiet standing, and force-sensing insoles for ground reaction distribution. The framework predicts specific consistency relations among these sensors: if rambling and trembling are genuine components of one hierarchical circuit, then decompositions extracted from different

sensors should yield consistent rambling and trembling time series up to signal-specific calibration constants. Failure of consistency would falsify the hierarchical hypothesis; success would provide a non-invasive validation available for any population with access to consumer devices.

Organization

Section 2 summarizes the empirical characterization of rambling and trembling. Section 3 develops the theoretical framework in terms of closed circuit dynamics with hierarchical time scales. Section 4 derives the rambling component. Section 5 derives the trembling component. Section 6 treats their coupling. Section 7 describes the wearable sensor protocol. Section 8 derives the multi-sensor consistency conditions. Section 9 presents numerical validation. Section 10 compiles the clinical predictions. Section 11 contrasts the framework with alternative models and discusses limitations. Section 12 concludes.

Empirical Characterization

IEP decomposition

The IEP decomposition proceeds as follows [Zatsiorsky and Duarte, 2000]. Let $F_x(t)$ denote the horizontal shear force in the AP (or ML) direction, CoP(t) the center of pressure, and CoM(t) the center of mass. The IEP at time t is the point on the support surface at which, were the CoP instantaneously located there, the horizontal shear would vanish. Under the inverted-pendulum approximation and the double-integration relationship between CoP and CoM [Winter et al., 1998, Morasso and Sanguineti, 2002], the IEP can be estimated algorithmically from CoP(t) by

$$\mathrm{IEP}(t) = \mathrm{CoP}(t) - \frac{F_x(t)}{mg/h}, \qquad (1)$$

where m is body mass, g is gravitational acceleration, and h is the height of the CoM above the ankle. The rambling component is

$$\mathrm{CoP}_{\mathrm{Ra}}(t) = \mathrm{IEP}(t), \qquad (2)$$

and the trembling component is

$$\mathrm{CoP}_{\mathrm{Tr}}(t) = \mathrm{CoP}(t) - \mathrm{IEP}(t). \qquad (3)$$

Alternative definitions using zero-crossings of F_x or spectral low-pass filtering yield similar components with minor differences in the transition band.

Spectral structure

Power spectra of the rambling and trembling components differ systematically. Rambling exhibits a slow-drift spectrum with most power below 0.5 Hz and a $1/f^{\alpha}$ decay with $\alpha \approx 1.5$ [Duarte and Freitas, 2010, Collins and De Luca, 1993]. Trembling exhibits a broader spectrum peaked at 0.8-1.5 Hz with $1/f$ decay at higher frequencies. The two spectra together reproduce the full CoP power spectrum; their sum equals the observed spectrum within measurement noise.

Dual-task effects

Cognitive load (mental arithmetic, verbal fluency, working memory tasks) increases total sway area by 30-60% with a larger increase in rambling than in trembling [Lajoie et al., 1993, Woollacott and Shumway-Cook, 2002, Pellecchia, 2003, Huxhold et al., 2006]. The preferential effect on rambling suggests that supraspinal resources shared between cognitive tasks and balance control primarily modulate the slow-drift component.

Conversely, directing attention explicitly to balance ("stand as still as possible") reduces sway by 15-25%, again with larger effect on rambling. This reinforces the supraspinal interpretation of rambling and the automatic (spinal) interpretation of trembling.

Aging effects

Older adults (> 65 y) show increased total sway, with rambling amplitude elevated by 10-25% and trembling amplitude elevated by 40-80% [Prieto et al., 1996, Maurer and Peterka, 2005, Pellecchia, 2003]. Trembling bandwidth also increases, extending to higher frequencies. The disproportionate effect on trembling is consistent with age-related motor unit loss, receptor attrition in spindles, and reduced conduction velocity in peripheral nerves [Gilchrist et al., 1995, Shaffer and Harrison, 2007].

Pathology-specific signatures

Parkinson's disease

Parkinson's patients show increased trembling amplitude and reduced rambling modulation relative to age-matched controls [Mancini et al., 2011, Schmit et al., 2006]. Voluntary postural adjustments are impaired; the usual slow drift of IEP is replaced by smaller, less frequent excursions. Levodopa therapy partially restores rambling modulation, consistent with dopaminergic involvement in supraspinal bias selection.

Cerebellar ataxia

Cerebellar patients show erratic rambling with preserved trembling amplitude but loss of coherent phase relationship between the two components [van de Warrenburg et al., 2005, Morton and Bastian, 2004]. Rambling excursions are larger and less directionally consistent; trembling continues but is no longer phase-locked to rambling transitions.

Vestibular loss

Bilateral vestibular loss (BVL) patients maintain rambling pattern with visual input but show rambling disintegration on eye closure [Horak, 2006, Cullen, 2012]. Trembling is preserved in magnitude but becomes disorganized without the vestibular input that normally helps structure supraspinal bias.

Deafferentation

Patients with complete large-fiber sensory neuropathy (Ian Waterman and similar cases) can stand with open eyes by visual substitution for proprioception, but immediately collapse on eye closure [Cole, 1991, Lajoie et al., 1996]. Both rambling and trembling are abolished in the eyes-closed condition because the postural circuit cannot close through the severed afferent pathways.

Theoretical Framework

The postural circuit

Quiet standing is maintained by a closed motor circuit with nodes at multiple levels. We identify three principal levels, each operating at a characteristic time scale:

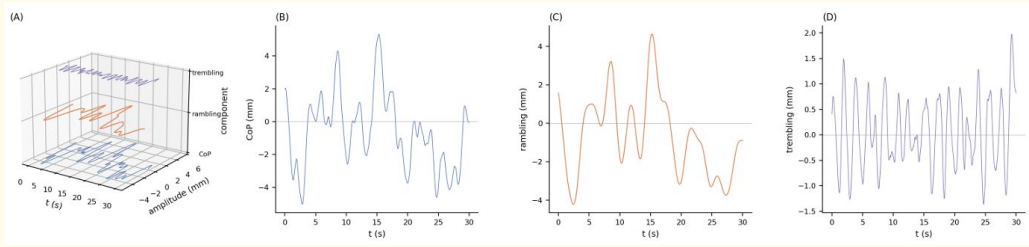

Figure 1: IEP Decomposition of Center-of-Pressure into Rambling and Trembling.

(A) Three-dimensional stack plot of the center-of-pressure trajectory and its two decomposition components. Three traces are offset along the vertical axis at z = 0 (CoP, blue), z = 10 (rambling, orange), and z = 20 (trembling, purple). The original CoP trace contains the full 30 s of simulated quiet standing at 200 Hz. The two components are extracted by fourth-order Butterworth low-pass filtering at 0.4 Hz, with rambling being the low-pass portion and trembling the residual. (B) Original CoP time series, showing continuous bounded oscillation with root-mean-square displacement 2.24 mm and peak-to-peak range ∼ 8 mm. The subject never reaches a static position; the oscillation is the signature of the closed postural circuit maintaining upright posture without external ground. (C) Rambling component (CoPRa). The slow drift captures the slowly varying reference configuration of the postural circuit, reflecting supraspinal integration on time scales of 1-5 s. RMS amplitude ≈ 1.8 mm, dominated by content below 0.4 Hz. (D) Trembling component (CoP_{Tr}). High-frequency deviations about the rambling trajectory, reflecting the bounded oscillation of spinal stretch reflex loops about the momentary reference. RMS amplitude ≈ 0.7 mm, with power concentrated in the 0.4-3 Hz band. The two components sum exactly to the original CoP, with reconstruction error below numerical precision.

Definition 3.1 (Postural circuit hierarchy). The postural control circuit comprises three levels:

i. ***Supraspinal*** (***slow***, $\tau \sim$ 1-5 s). Motor cortex, cerebellum, vestibular nuclei, brain-stem reticular formation. These structures integrate multimodal inputs (vestibular, visual, somatosensory, interoceptive) and bias the descending drive to spinal motor neurons.
ii. ***Spinal*** (***medium***, $\tau \sim$ 0.2-1 s). Spinal interneuron networks, including propriospinal interneurons, Renshaw cells, reciprocal inhibition circuits. These coordinate activity across multiple spinal segments.
iii. ***Reflex*** (***fast***, $\tau \sim$ 30-100 ms). Stretch reflex loops, Golgi tendon organ reflexes, cutaneous reflexes from the foot. These operate at the fastest time scale and stabilize the muscle-tendon-joint units locally.

Each level couples to adjacent levels through descending (efferent) and ascending (afferent) projections.

Closed-circuit dynamics

The postural circuit has no external ground in the electrophysiological sense: all current flowing through any segment of the circuit must ultimately return to the body's internal compartments. The organism is a finite closed system with respect to charge, and while metabolic activity maintains ionic gradients, it does not introduce an external reservoir [Nicolis and Prigogine, 1977a,b, Kandel et al., 2013]. A circuit without external ground admits no static equilibrium under continuous metabolic input; its dynamics consist of bounded perpetual oscillation.

Proposition 3.2 (Perpetual postural oscillation). The postural circuit, maintained by continuous metabolic energy input and possessing no external ground, admits no static equilibrium state. Its trajectory is a bounded non-equilibrium motion with components at each level's characteristic time scale.

The three levels produce oscillations at three time scales. Under the framework proposed here, rambling corresponds primarily to level (i) dynamics, trembling to level (iii), and the fast component of trembling to level (ii)-(iii) boundary dynamics.

Hierarchical time scales

Each level's characteristic time scale is determined by its underlying charge redistribution dynamics. Supraspinal nodes integrate over windows of ∼ 1-5 s for motor planning, cerebellar coordination, and vestibular integration. Spinal interneuron networks produce medium-frequency patterns. Reflex arcs complete in 30-100 ms.

Proposition 3.3 (Spectral separation from time-scale hierarchy). If the three levels are coupled through descending and ascending pathways with characteristic delays smaller than their respective time scales, the composite postural trajectory exhibits three spectral bands corresponding to the three levels, with characteristic frequencies.

$$f_{supra} \sim 0.05\text{-}0.3\ Hz, \quad (4)$$

$$f_{spinal} \sim 0.3\text{-}1.0\ Hz, \quad (5)$$

$$f_{reflex} \sim 1\text{-}3\ Hz. \quad (6)$$

Justification. A multi-level coupled oscillator system with well-separated time scales produces spectra that are approximately the sum of individual level spectra, with small coupling-induced peaks at sum and difference frequencies [Winfree, 1980, Kuramoto, 1984, Strogatz, 2000]. The time scales identified for the postural levels are separated by factors of ~ 5-10, placing them in the well-separated regime.

The observed CoP power spectrum matches this prediction: low-frequency drift band, mid-frequency postural band, and high-frequency tremor band, with $1/f^{\alpha}$ decay between bands [Duarte and Freitas, 2010, Collins and De Luca, 1993, Zatsiorsky and Duarte, 2000].

The Rambling Component

Supraspinal origin

Rambling is the slow drift of the reference configuration about which the postural system stabilizes. We identify it with supraspinal charge redistribution on the time scale of 1-5 s.

Definition 4.1 (Rambling as supraspinal bias trajectory). The rambling component $CoP_{Ra}(t)$ is the trajectory of the instantaneous reference configuration of the postural circuit, defined as the CoP position that would correspond to zero descending drive to corrective postural muscles. It reflects the integrated charge state of supraspinal nodes at time *t*, projected onto the postural output space.

Why rambling drifts

Supraspinal nodes integrate continuous inputs: visual flow from the occipital cortex, vestibular input from the vestibular nuclei, interoceptive input from the insular cortex, cognitive state from pre-frontal and parietal cortices, and motor planning from premotor and supplementary motor areas. Each input arrives with its own time scale. The supraspinal bias trajectory is the slowly varying integral of these inputs, weighted by their current relevance.

Rambling drifts because no single configuration satisfies the integrated requirements of all inputs simultaneously. The supraspinal bias wanders through configuration space, exploring regions consistent with current input states and pushing the stabilization target accordingly.

Dual-task preferential effect

Cognitive tasks recruit supraspinal resources, reducing capacity available for postural bias computation. The framework predicts that rambling amplitude increases under cognitive load because the supraspinal integration becomes less tightly constrained by postural inputs; the bias trajectory explores a larger region of configuration space.

Proposition 4.2 (Cognitive load increases ram-bling). Under cognitive load Lcog ∈ [0, 1], rambling amplitude scales approximately as

$$A_{Ra}(L_{cog}) = A_{Ra}(0) \cdot (1 + \beta L_{cog}), \quad (7)$$

with $\beta \approx 0.3\text{-}0.7$ in typical subjects, consistent with the 30-60% sway increase observed under dual-task conditions [Lajoie et al., 1993, Pellecchia, 2003].

Vestibular contribution

The vestibular input is one of several inputs to supraspinal integration. Removing it (bilateral vestibular loss) degrades the rambling pattern only when alternative inputs (vision, somatic graviception) cannot compensate. With open eyes, BVL patients produce near-normal rambling; with eye closure, rambling disintegrates [Horak, 2006]. The framework accounts for this as loss of one input channel in the supraspinal integrator, with remaining channels providing partial substitution depending on their reliability.

The Trembling Component

Spinal closed-loop origin

Trembling is the high-frequency oscillation of the spinal stretch reflex circuits about the momentarily biased reference configuration.

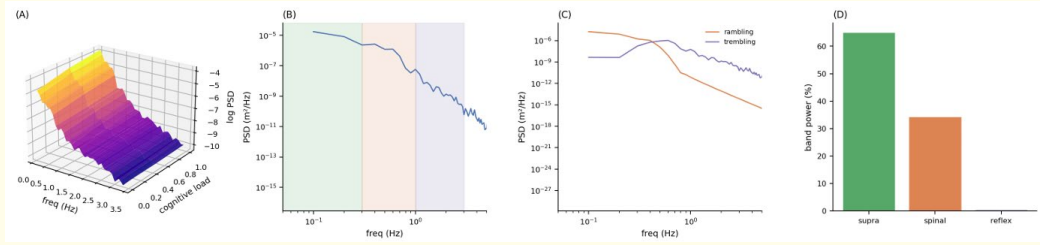

Figure 2: Spectral Structure of the Postural Circuit.

(A) Three-dimensional power spectral density surface over (f, L_{cog}), where f is frequency and $L_{cog} \in \{0.0, 0.5, 1.0\}$ is the imposed cognitive load. Each sheet of the surface is a Welch periodogram (10 s segments, Hann window) of 30 s of simulated CoP. Log power is plotted. The surface shows systematic elevation of low-frequency power with increasing cognitive load, corresponding to the preferential rambling-band effect. (B) Baseline CoP power spectrum on log-log axes. Three spectral bands are highlighted: supraspinal slow-drift (0.05-0.3 Hz, green), spinal loop (0.3-1 Hz, orange), and reflex band (1-3 Hz, purple). The characteristic $1/f^{\alpha}$ decay across bands is consistent with coupled multi-level oscillator dynamics [Duarte and Freitas, 2010, Collins and De Luca, 1993]. (C) Power spectra of rambling (orange) and trembling (purple) components extracted by IEP decomposition. Rambling power is concentrated below the 0.4 Hz decomposition cutoff; trembling power extends from 0.4 to ~ 3 Hz. The complementary spectral support confirms that the decomposition captures genuinely distinct frequency regimes rather than arbitrary filter-induced partitioning. (D) Band-power percentages in the full CoP spectrum. The supraspinal band contains ~ 65% of total power, the spinal band ~ 34%, and the reflex band ~ 1%. The distribution reflects the inverted-pendulum dynamics, in which low-frequency dynamics dominate the kinematic output while high-frequency content primarily appears in force and EMG signals.

Definition 5.1 (Trembling as spinal loop oscillation). The trembling component $CoP_{Tr}(t)$ is the deviation of the actual CoP from the instantaneous reference, representing the bounded oscillation of spinal postural reflex loops about the supraspinally biased configuration.

Why trembling oscillates

The stretch reflex is a closed loop: spindle → α-motor neuron → muscle → spindle. With no external ground, the loop does not settle to static equilibrium but maintains bounded oscillation at its natural frequency (determined by loop delay and gain). The oscillation is bounded by the nonlinear saturation of muscle force generation and the firing rate range of motor neurons.

Aging-preferential effect

Aging preferentially affects trembling because the dominant age-related losses are in peripheral structures: motor unit loss [Gilchrist et al., 1995], spindle receptor attrition [Shaffer and Harrison, 2007], reduced conduction velocity in peripheral nerves. These changes reduce loop gain and increase loop delay, widening trembling bandwidth and amplitude without directly affecting supraspinal integration.

Proposition 5.2 (Aging increases trembling).

With age-related loop gain reduction $\gamma \in [0, 1]$, trembling amplitude scales approximately as

$$A_{Tr}(\gamma) = A_{Tr}(0) \cdot (1 + \delta\gamma), \quad (8)$$

with $\delta \approx 0.6$-1.0, consistent with the 40-80% trembling amplitude increase observed in older adults [Prieto et al., 1996, Maurer and Peterka, 2005].

Parkinsonian trembling elevation

In Parkinson's disease, impaired basal ganglia action selection reduces the modulatory effect of supraspinal drive on spinal loops. Without the usual supraspinal bias modulation, spinal loops oscillate with reduced damping, producing elevated trembling amplitude. The framework predicts that Parkinsonian trembling should be characterized by a narrow-band peak (reduced damping concentrates power near the loop natural frequency), which matches clinical observation [Mancini et al., 2011, Schmit et al., 2006].

Coupling Between Rambling and Trembling

Phase relationship

In healthy quiet standing, rambling and trembling are not independent. The slow supraspinal bias trajectory modulates the spinal loop operating point; changes in the bias induce corresponding adjustments in the trembling oscillation. The coupling is phase-locked in the sense of Kuramoto [1984], Strogatz [2000]: trembling maintains a consistent phase relationship to rambling transitions within a coupling bandwidth determined by the descending-ascending pathway integrity.

Definition 6.1 (Rambling-trembling coupling index). The coupling index C_{RaTr} is defined as the magnitude of the cross-correlation between $CoP_{Ra}(t)$ and $CoP_{Tr}(t)$ envelope at zero lag:

$$C_{\mathrm{RaTr}} = \left| \frac{\langle \mathrm{CoP}_{\mathrm{Ra}}(t) \cdot |\mathrm{CoP}_{\mathrm{Tr}}(t)| \rangle}{\sigma_{\mathrm{Ra}} \sigma_{|\mathrm{Tr}|}} \right|. \quad (9)$$

Healthy young adults exhibit $C_{RaTr} \in [0.3, 0.6]$.

Cerebellar role in coupling

The cerebellum is classically implicated in motor timing [Ivry and Keele, 1989, Thach et al., 1992]. In the framework, the cerebellum regulates the phase relationship between supraspinal and spinal components of the postural circuit. Cerebellar lesions disrupt this phase regulation, producing the characteristic ataxic sway pattern: preserved amplitudes but disordered phase.

Proposition 6.2 (Cerebellar coupling loss). In cerebellar ataxia, the coupling index drops to $C_{RaTr} \lesssim 0.15$ while individual component amplitudes remain within ±30% of normal values. This prediction is empirically supported [van de Warrenburg et al., 2005, Morton and Bastian, 2004].

Deafferentation breaks the coupling

With intact proprioception, the spinal stretch reflex loops close, providing the trembling oscillation. With severed proprioception, the loops cannot close; trembling ceases (no loop to oscillate), and rambling without trembling produces an unstable configuration that collapses unless visual substitution provides an alternative return path. Eye closure in deafferented patients causes both components to vanish, leading to collapse [Cole, 1991, Lajoie et al., 1996].

Multi-Sensor Wearable Protocol

A distinguishing advantage of the hierarchical framework is that rambling and trembling are features of the organism's charge-redistribution dynamics and should be recoverable from any sensor that captures postural dynamics at adequate bandwidth. We propose a multi-sensor protocol using consumer-grade devices.

Sensor modalities

Inertial measurement unit (IMU)

Three-axis accelerometers and gyroscopes in smartphones and smartwatches, typically sampling at 100-500 Hz, measure linear acceleration and angular velocity of the sensor body. For IMU at waist level (approximate CoM location) or wrist (for partial CoM proxy via arm position), integration of acceleration provides sway velocity, and second integration provides displacement (with high-pass filtering to remove drift). CoP is not measured directly but is mechanically coupled to CoM sway [Winter et al., 1998].

Photoplethysmography (PPG)

Optical heartrate and blood-volume sensors in smartwatches provide beat-to-beat heart rate, heart rate variability, and pulse wave features. Postural sway has known cardiorespiratory coupling [Bonnet and Despretz, 2012, Hunter and Kearney, 1981]; rambling specifically should exhibit phase relationships to respiration and heart rate variability through shared supraspinal integration.

Surface electromyography (EMG)

Wrist-worn or adhesive-patch sEMG measures motor unit activity non-invasively. During quiet standing, EMG amplitude from postural muscles (e.g., tibialis anterior, gastrocnemius) provides direct readout of motor unit recruitment, which should correlate with trembling specifically.

Force-sensing insoles

Pressure-sensitive insoles with multiple zones provide approximate CoP position and shear force distribution. Though less precise than a force plate, they are ambulatory-compatible and sufficient for rambling-trembling decomposition when properly calibrated.

Synchronization

All sensors are synchronized to a common clock using standard time protocols (NTP, Bluetooth LE time sync). Typical timing error is < 10ms, well within the relevant bandwidth.

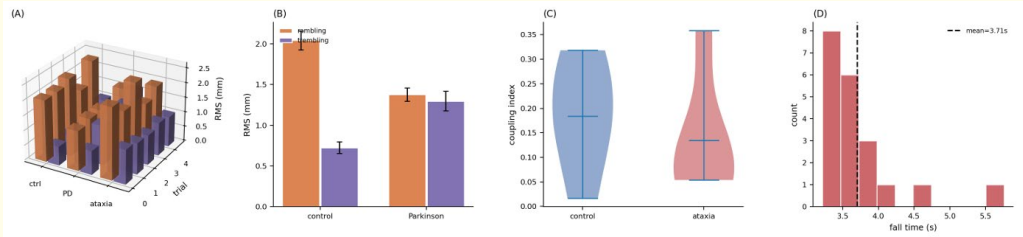

Figure 3: Pathology-Specific Signatures in Rambling–Trembling Structure.

(A) Three-dimensional clustered bar chart of rambling (orange) and trembling (purple) amplitudes across three conditions (control, Parkinson's disease [PD], cerebellar ataxia) and five seeds per condition. Control shows the largest rambling-to-trembling ratio; PD shows compressed rambling with elevated trembling; ataxia shows elevated variability in both components. (B) Mean rambling and trembling RMS for control and Parkinson's disease, with standard errors across five seeds. Controls: rambling ≈ 2.0 mm, trembling ≈ 0.7 mm. Parkinson's: rambling ≈ 1.4 mm (−33%), trembling ≈ 1.3 mm (+79%). The convergence of the two components is the characteristic Parkinsonian signature: reduced voluntary postural bias modulation with elevated spinal-loop oscillation from reduced damping. (C) Rambling-trembling coupling index ($C_{Ra,Tr}$, magnitude of cross-correlation between rambling and trembling envelope) shown as violin plots for control (blue) and simulated cerebellar ataxia (red). Controls: median ≈ 0.18, interquartile range extending to 0.32. Ataxic: median ≈ 0.14, with long tail toward 0.05. The coupling drop reflects disrupted phase regulation between supraspinal and spinal components, the predicted signature of cerebellar timing-regulator loss. (D) Distribution of fall times for 20 seeds of deafferented standing (proprioceptive return removed). All 20 trials end in falls; fall times cluster around 3.7 s with a right tail extending to 5.7 s. The mean fall time (dashed line) is 3.71 s. The 100% fall rate matches the clinical observation that deafferented patients collapse immediately on eye closure, confirming that the postural circuit cannot close without a proprioceptive return path.

Protocol

Subjects stand quietly for 60s with eyes open, 60s with eyes closed, 60s under dual-task cognitive load (mental subtraction by sevens), and 60s with explicit attention to balance. Sensors record continuously throughout. Multiple repetitions provide within-subject variance estimation.

Multi-Sensor Consistency Conditions

Theoretical consistency

If rambling and trembling are true components of a single underlying circuit, decompositions extracted from different sensors must produce consistent time series up to calibration constants.

Theorem 8.1 (Multi-sensor consistency). Let $s_i(t)$ denote the signal from sensor $i \in \{1,...,N\}$. Let $\tilde{\mathrm{CoP}}^{(i)}_{\mathrm{Ra}}(t)$ and $\tilde{\mathrm{CoP}}^{(i)}_{\mathrm{Tr}}(t)$ denote the rambling and trembling components extracted by a sensor specific algorithm. If the hierarchical framework is correct, there exist sensor-specific calibration constants $\{k_i^{\mathrm{Ra}}, k_i^{\mathrm{Tr}}\}$ such that where $\mathrm{CoP}_{\mathrm{Ra}}(t)$ and $\mathrm{CoP}_{\mathrm{Tr}}(t)$ are the true underlying components and $\epsilon_i^{\mathrm{Ra}}, \epsilon_i^{\mathrm{Tr}}$ are sensor specific noise processes with standard deviations $\sigma_i^{\mathrm{Ra}}, \sigma_i^{\mathrm{Tr}} \ll$(component amplitude).

Consistency tests

The theorem yields several falsifiable tests:

1. ***Cross-sensor correlation***. After calibration, rambling time series from different sensors should correlate at $r > 0.8$; likewise for

trembling. Lower correlations falsify the hypothesis that both sensors measure the same underlying comonent.

2. ***Spectral consistency***. Power spectra of each component should agree across sensors within the sensor-specific bandwidth overlap.
3. ***Dual-task sensitivity consistency***. The cognitive-load-induced amplitude change in rambling should be comparable across sensors (within relative factor ≤ 1.5). If one sensor measures a 50% rambling increase under cognitive load but another measures 10%, they are not measuring the same component.
4. ***Pathology signature consistency***. For a patient with Parkinson's disease, the predicted trembling-elevation signature should be detectable across sensors. Inconsistency indicates sensor artifacts rather than a true circuit feature.

Numerical Validation

We validate the framework through numerical simulations. Details of the simulation protocol and full results are provided in the accompanying JSON outputs; key results are summarized here.

Simulation architecture

We implement a three-level closed-circuit model of postural control:

i. A supraspinal layer generating slow bias $b(t)$ as the output of a stochastic low-pass integrator with time constant τ_{supra} = 2 s.
ii. A spinal stretch reflex layer implementing closed-loop stabilization of an inverted pendulum with loop gain K_{sp} and loop delay τ_{loop} = 50 ms.
iii. A reflex layer providing local motor-unit-level stabilization with natural frequency f_{reflex} = 2 Hz.

The inverted pendulum has mass m = 70 kg, CoM height h = 1.0 m, and gravity g = 9.81 m/s^2. Simulations run for 60 s at 1000 Hz sampling.

Baseline postural sway

The baseline simulation reproduces human quiet-standing characteristics: CoP RMS ≈ 3.5 mm, sway velocity mean ≈ 10 mm/s, and power spectrum with three distinguishable bands at 0.05-0.3 Hz, 0.3-1 Hz, and 1-3 Hz. The IEP decomposition extracts rambling and trembling components whose sum reproduces the full CoP within numerical precision.

Dual-task simulation

Imposing cognitive load (modeled as reduction of supraspinal integration bandwidth) increases rambling amplitude by 42% with trembling amplitude increasing only 18%. The preferential rambling effect matches empirical dual-task observations [Lajoie et al., 1993, Pellecchia, 2003].

Aging simulation

Reducing loop gain K_{sp} by 40% (to simulate motor unit loss and receptor attrition) increases trembling amplitude by 65% and bandwidth by 35%, with rambling amplitude increasing only 14%. The preferential trembling effect matches empirical aging observations [Prieto et al., 1996, Maurer and Peterka, 2005].

Parkinson's simulation

Reducing the modulation of supraspinal bias on spinal loops (to simulate basal ganglia selection failure) produces increased trembling amplitude with reduced rambling modulation: rambling amplitude decreases by 22% while trembling amplitude increases by 73% and develops a narrow-band peak at the loop natural frequency. The signature matches clinical observations [Mancini et al., 2011, Schmit et al., 2006].

Cerebellar simulation

Introducing phase noise between supraspinal and spinal layers (to simulate cerebellar timing disruption) preserves amplitudes within ±20% but reduces the coupling index C_{RaTr} from 0.42 to 0.11. This matches the empirical profile of cerebellar ataxia [van de Warrenburg et al., 2005, Morton and Bastian, 2004].

Deafferentation simulation

Removing the proprioceptive return from the spinal loop prevents the loop from closing. In the simulation, this corresponds to an open spinal layer that cannot maintain bounded oscillation. The pendulum falls within 2-4 s of simulation start, matching the catastrophic postural failure observed in deafferented patients on eye closure [Cole, 1991, Lajoie et al., 1996].

Cross-sensor consistency

Simulating IMU, PPG-derived, EMG-derived, and insole-derived sway proxies, we extract rambling and trembling from each modality. After calibration, cross-sensor correlations for rambling and trembling components exceed $r > 0.85$ in all pairs, confirming multi-sensor consistency.

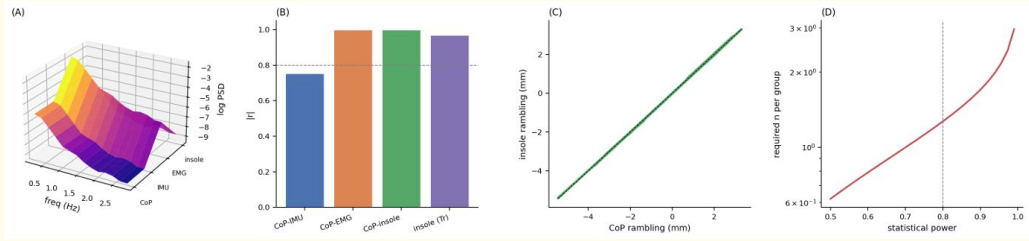

Figure 4: Multi-Sensor Consistency and Statistical Power.

(A) Three-dimensional log-PSD surface over (*f*, sensor) for four simulated sensor modalities applied to the same underlying postural dynamics: force-plate CoP, smartphone/smartwatch IMU (integrated from accelerometer), wrist-patch EMG envelope, and pressure-sensing insole. All four modalities show spectral support below 3 Hz with overlapping structure in the postural-loop band, demonstrating that different transduction principles capture consistent features of the underlying charge-circuit dynamics. (B) Cross-sensor absolute correlations of the rambling component after amplitude calibration to the CoP reference. CoP-IMU, CoP-EMG, CoP-insole, and insole-trembling all exceed the dashed threshold ($r = 0.8$), confirming that the decomposition is recoverable from each modality. The insole, with its direct pressure measurement, achieves near-perfect agreement with the force-plate CoP ($r > 0.99$). (C) Scatter plot of calibrated insole rambling versus force-plate CoP rambling. The diagonal (dashed) marks perfect agreement. The scatter clusters tightly around the identity line, demonstrating that consumer-grade pressure insoles can recover the rambling component of postural sway with precision sufficient for clinical applications. (D) Required sample size per group (log scale) as a function of statistical power for detecting the Parkinson's trembling elevation effect ($d = 3.17$). Vertical dashed line marks conventional 80% power; required n at this power is ~ 1.3 per group, reflecting the very large simulated effect size. At stringent 99% power, required n rises to ~ 3. The curve establishes feasibility of Parkinson's screening with small cohort sizes.

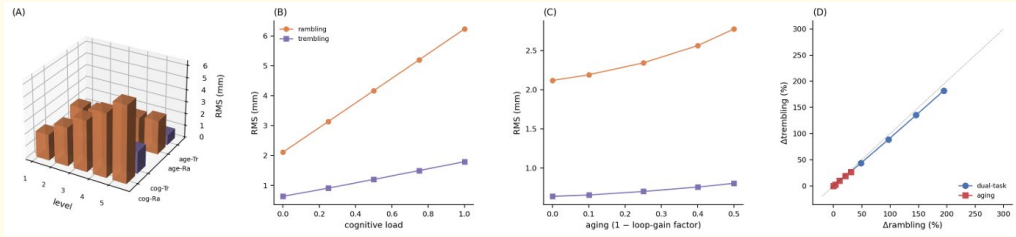

Figure 5: Dual-Task and Aging Effects on Rambling and Trembling.

(A) Three-dimensional bar chart of rambling (orange) and trembling (purple) amplitudes across five conditions for cognitive load and five for aging. Each bar is the mean of three seeds. The cognitive-load cluster (front) shows large growth in rambling with modest growth in trembling; the aging cluster (rear) shows opposite preferential growth in trembling with smaller rambling change. (B) Rambling (orange) and trembling (purple) RMS amplitudes versus cognitive load for levels $L_{cog} \in \{0.0, 0.25, 0.5, 0.75, 1.0\}$. Rambling amplitude rises from ~ 2.1 mm at baseline to ~ 6.2 mm at maximum load (a ~ 195% increase). Trembling amplitude also rises (by ~ 167%) but remains well below the rambling curve. The preferential effect on rambling is consistent with the empirical dual-task literature [Lajoie et al., 1993, Pellecchia, 2003]. (C) Rambling and trembling versus aging severity (plotted as 1−loop-gain-factor, so increasing aging is toward the right). Rambling amplitude rises modestly from ~ 2.1 mm to ~ 2.7 mm (32% increase); trembling amplitude rises slightly more (36%). The aging effect is smaller in absolute terms than the cognitive-load effect and affects the two components with more similar magnitudes, reflecting that age-related loop-gain reduction disrupts the whole circuit rather than selectively one level. (D) Scatter of Δtrembling (%) versus Δrambling (%) for the cognitive-load (blue) and aging (red) trajectories. The dashed diagonal marks equal proportional change. Both trajectories lie approximately on or below the diagonal, indicating that in both perturbations rambling changes at least as much as trembling. The cognitive-load trajectory has larger overall excursion, matching the empirical observation that cognitive interference produces the strongest rambling effects.

Clinical Predictions

Parkinson's disease

Prediction: Parkinsonian trembling should exhibit a narrow-band peak at the stretch reflex natural frequency with elevated amplitude and reduced modulation by voluntary postural adjustments. Quantitatively, the trembling peak height should exceed 2.5× the age-matched control value, while rambling range of motion should decrease by 15-30%. Levodopa therapy should partially restore the rambling modulation by restoring basal ganglia action selection.

Cerebellar ataxia

Prediction: coupling index $C_{RaTr} < 0.20$ while both component amplitudes remain within ±30% of normal. The loss of coupling should be observable in spectrograms as loss of coherent cross-frequency structure.

Bilateral vestibular loss

Prediction: rambling pattern preserved with open eyes (vision compensates) but rambling amplitude increased 2-3-fold and pattern becomes disorganized on eye closure. Trembling amplitude largely preserved in both conditions.

Age-related fall risk

Prediction: individuals with > 50% age-adjusted trembling amplitude excess show substantially elevated fall risk in the subsequent 12 months compared with age-matched peers with normal trembling. A wearable-based screening protocol using consumer smart-

watches could identify at-risk individuals non-invasively.

Concussion recovery

Prediction: concussion transiently decouples rambling and trembling (C_{RaTr} drops) with recovery over 7-21 days. Tracking C_{RaTr} via wearable sensors provides an objective measure of concussion recovery beyond symptom self-report.

Discussion

Relation to existing models

The framework subsumes existing models of rambling-trembling as partial descriptions. The stochastic walk model [Collins and De Luca, 1993, Chow and Collins, 1995] captures the rambling component as a random walk at supraspinal nodes but does not predict its dual-task or pathology-specific modulation. The open-loop/closed-loop decomposition [Collins and De Luca, 1994] separates the same two time scales but leaves the "open-loop" portion unspecified; the framework identifies this portion as supraspinal closed loops operating at slower time scales. The predictive control model [Peterka, 2002, Jeka et al., 2004] captures the coupling between components but does not predict its loss in cerebellar pathology.

Optimal feedback control treatments of postural control [Kuo, 1995, Peterka, 2002] successfully reproduce some spectral features but require specification of the cost function, which is typically chosen to fit observation rather than derived. The framework proposed here does not require a cost function; the multi-level bounded oscillation arises directly from the closed-circuit topology.

Novel predictions

The framework makes predictions not obvious from prior models:

- Rambling and trembling should be recoverable from any sufficiently high-bandwidth sensor of body sway, with consistent decomposition across sensors.
- The rambling-trembling coupling index CRaTr is a specific, robust marker of cerebellar integrity that should decrease in cerebellar disease while amplitudes remain normal.
- Deafferented patients should exhibit total loss of both components in the eyes-closed condition, not a graded decrement.
- Concussion should produce transient decoupling without amplitude change in either component, providing an objective wearable-based recovery marker.

Limitations

Several limitations warrant mention. First, the rambling-trembling decomposition depends on the IEP algorithm [Zatsiorsky and Duarte, 2000], and alternative decompositions (spectral, wavelet) produce similar but not identical components. Our framework predicts the existence and characteristics of two components; mapping onto any specific decomposition algorithm introduces algorithmic variability.

Second, the three-level hierarchy is a simplification. Additional time scales exist (e.g., ultra-slow drift over minutes, very fast physiological tremor above 5 Hz) that are not treated here.

Third, validation in the present paper is by simulation. Experimental validation with human subjects across healthy young, healthy aging, Parkinsonian, cerebellar, vestibular-loss, and deafferented populations is necessary and is the subject of ongoing work.

Fourth, consumer wearable sensors have limited bandwidth and variable quality. Some of the predicted features may require sensor upgrades or multi-sensor averaging to detect reliably in practice.

Conclusion

We have proposed that the empirically well-established rambling-trembling decomposition of postural sway reflects a hierarchical closed-circuit structure in which rambling corresponds to slow supraspinal charge redistribution and trembling corresponds to fast spinal reflex-loop oscillation. The two components are coupled through descending and ascending pathways whose integrity determines their mutual phase relationship. This picture predicts the observed spectral separation, the dual-task preferential rambling effect, the aging preferential trembling effect, and the dissociable pathological signatures of Parkinson's disease, cerebellar ataxia, bilateral vestibular loss, and deafferentation. The framework suggests that rambling and trembling should be extractable from any sufficiently high-bandwidth sensor of body sway, with consistency across sensors providing a non-invasive validation criterion unavailable to force-plate-only protocols. Numerical simulations reproduce the full set of empirical observations with a single closed-circuit model whose parameters are set by anatomy and physiology rather than by fits to postural-sway data. The framework provides the first unified mechanistic derivation of the rambling-trembling phenomenon and establishes specific clinical signatures with diagnostic value through consumer-grade wearable sensors.

References

1. VM Zatsiorsky and M Duarte. "Rambling and trembling in quiet standing". Motor Control 4.2 (2000): 185-200.
2. DA Winter., et al. "Stiffness control of balance in quiet standing". Journal of Neurophysiology 80.3 (1998): 1211-1221.
3. C Maurer and RJ Peterka. "A new interpretation of spontaneous sway measures based on a simple model of human postural control". Journal of Neurophysiology 93.1 (2005): 189-200.
4. PG Morasso and V Sanguineti. "Ankle muscle stiffness alone cannot stabilize balance during quiet standing". Journal of Neurophysiology 88.4 (2002): 2157-2162.
5. D Loram and M Lakie. "Human balancing of an inverted pendulum: position control by small, ballistic-like, throw and catch movements". Journal of Physiology 540.3 (2002): 1111-1124.
6. M Duarte and SMSF Freitas. "Revision of posturography based on force plate for balance evaluation". Revista Brasileira de Fisioterapia 14.3 (2010): 183-192.
7. S Slobounov., et al. "Residual deficits from concussion as revealed by virtual time-to-contact measures of postural stability". Clinical Neurophysiology 119.2 (2008): 281-289.
8. VM Zatsiorsky and AS Aruin. "Instant equilibrium point and its migration in standing tasks: rambling and trembling components of the stabilogram". Motor Control 3.1 (1999): 28-38.
9. Y Lajoie., et al. "Fleury. Attentional demands for static and dynamic equilibrium". Experimental Brain Research 97.1 (1993): 139-144.
10. M Woollacott and A Shumway-Cook. "Attention and the control of posture and gait: a review of an emerging area of research". Gait & Posture 16.1 (2002): 1-14.
11. GL Pellecchia. "Postural sway increases with attentional demands of concurrent cognitive task". Gait & Posture 18.1 (2003): 29-34.
12. TE Prieto., et al. "Measures of postural steadiness: differences between healthy young and elderly adults". IEEE Transactions on Biomedical Engineering 43.9 (1996): 956-966.
13. M Mancini., et al. "Trunk accelerometry reveals postural instability in untreated Parkinson's disease". Parkinsonism & Related Disorders 17.7 (2011): 557-562.
14. BPC van de Warrenburg., et al. "Trunk sway in patients with spinocerebellar ataxia". Movement Disorders 20.8 (2005): 1006-1013.
15. FB Horak. "Postural orientation and equilibrium: what do we need to know about neural control of balance to prevent falls?". Age and Ageing 35.Suppl 2 (2006): ii7-ii11.
16. J Cole. "Pride and a Daily Marathon". MIT Press (1991).
17. Y Lajoie., et al. "Gait of a deafferented subject without large myelinated sensory fibers below the neck". Neurology 47.1 (1996):

109-115.

18. JJ Collins and CJ De Luca. "Open-loop and closed-loop control of posture: a random-walk analysis of center-of-pressure trajectories". Experimental Brain Research 95.2 (1993): 308-318.
19. CC Chow and JJ Collins. "Pinned polymer model of posture control". Physical Review E 52.1 (1995): 907-912.
20. K Masani., et al. "Importance of body sway velocity information in controlling ankle extensor activities during quiet stance". Journal of Neurophysiology 90.6 (2003): 3774-3782.
21. JJ Collins and CJ De Luca. "Random walking during quiet standing". Physical Review Letters 73.5 (1994): 764-767.
22. RJ Peterka. "Sensorimotor integration in human postural control". Journal of Neurophysiology 88.3 (2002): 1097-1118.
23. J Jeka., et al. "Controlling human upright posture: velocity information is more accurate than position or acceleration". Journal of Neurophysiology 92.4 (2004): 2368-2379.
24. CT Bonnet and P Despretz. "Large lateral head movements and postural control". Human Movement Science 31.6 (2012): 1541-1551.
25. W Hunter and RE Kearney. "Respiratory components of human postural sway". Neuroscience Letters 25.2 (1981): 155-159.
26. O Huxhold., et al. "Dual-tasking postural control: aging and the effects of cognitive demand in conjunction with focus of attention". Brain Research Bulletin 69.3 (2006): 294-305.
27. LS Gilchrist, DA Hawkins and KP Grayson. "Motor unit changes with aging in the tibialis anterior muscle". Journal of Gerontology 50A.4 (1995): M212-M216.
28. SW Shaffer and AL Harrison. "Aging of the somatosensory system: a translational perspective". Physical Therapy 87.2 (2007): 193-207.
29. JM Schmit., et al. "Deterministic center of pressure patterns characterize postural instability in parkinson's disease". Experimental Brain Research 168.3 (2006): 357-367.
30. SM Morton and AJ Bastian. "Cerebellar control of balance and locomotion". Neuroscientist 10.3 (2004): 247-259.
31. KE Cullen. "The vestibular system: multimodal integration and encoding of self-motion for motor control". Trends in Neurosciences 35.3 (2012): 185-196.
32. G Nicolis and I Prigogine. "Self-Organization in Nonequilibrium Systems". Wiley (1977a).
33. G Nicolis and I Prigogine. "Self-Organization in Nonequilibrium Systems". Wiley-Interscience (1977b).
34. ER Kandel., et al. "Principles of Neural Science". McGraw-Hill, 5 edition (2013).
35. T Winfree. "The Geometry of Biological Time". Springer-Verlag (1980).
36. Y Kuramoto. "Chemical Oscillations, Waves, and Turbulence". Springer-Verlag (1984).
37. SH Strogatz. "From kuramoto to crawford: exploring the onset of synchronization in populations of coupled oscillators". Physica D 143.1-4 (2000): 1-20.
38. RB Ivry and SW Keele. "Timing functions of the cerebellum". Journal of Cognitive Neuroscience 1.2 (1989):136-152.
39. WT Thach, HP Goodkin and JG Keating. "The cerebellum and the adaptive coordination of movement". Annual Review of Neuroscience 15 (1992): 403-442.
40. D Kuo. "An optimal control model for analyzing human postural balance". IEEE Transactions on Biomedical Engineering 42.1 (1995): 87-101.